

Dense Pixel-wise Micro-motion Estimation of Object Surface by using Low Dimensional Embedding of Laser Speckle Pattern

Ryusuke Sagawa¹[0000-0002-6778-8838], Yusuke Higuchi²,
Hiroshi Kawasaki²[0000-0001-5825-6066], Ryo Furukawa³[0000-0002-2063-1008],
and Takahiro Ito¹[0000-0003-2886-1067]

¹ National Institute of Advanced Industrial Science and Technology

² Kyushu University

³ Hiroshima City University

Abstract. This paper proposes a method of estimating micro-motion of an object at each pixel that is too small to detect under a common setup of camera and illumination. The method introduces an active-lighting approach to make the motion visually detectable. The approach is based on speckle pattern, which is produced by the mutual interference of laser light on object's surface and continuously changes its appearance according to the out-of-plane motion of the surface. In addition, speckle pattern becomes uncorrelated with large motion. To compensate such micro- and large motion, the method estimates the motion parameters up to scale at each pixel by nonlinear embedding of the speckle pattern into low-dimensional space. The out-of-plane motion is calculated by making the motion parameters spatially consistent across the image. In the experiments, the proposed method is compared with other measuring devices to prove the effectiveness of the method.

1 Introduction

The analysis of physical minute movements of objects is important to understand the behavior of various systems including mechanical systems, fluids analysis and biological studies. For example, mechanical systems vibrate at various frequency distributed over a wide range from several hertz to several kilohertz only with the extremely small amplitude, such as less than one millimeter. There are many approaches to measure such a minute movements, and typical methods are to use vibration sensors based on various measurement principles including accelerometers and displacement gauges. Although these methods can measure such a minute movements precisely, there is a severe limitation, such as only a single point can be measured by each sensor, because of necessity of physical contact, resulting in a measurement of only limited and small areas. In order to conduct accurate and robust analysis on spatio and temporal effect of vibration, measurement of micro movement of dense and wide region is required, which cannot be achieved by existing sensors and methods.

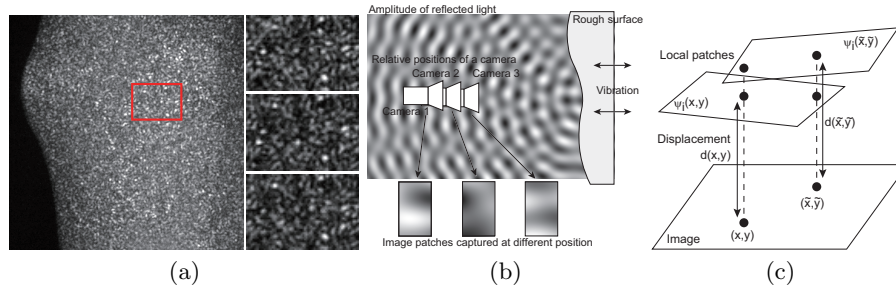


Fig. 1. An example of speckle pattern and modeling motion of piecewise planes. (a) An example of speckle pattern on an object’s surface is shown. While the power of the incident light is uniform, the dotted pattern is observed by a camera. (b) The amplitude of light changes drastically according to the position due to the mutual interference. (c) The plane parameters $\psi_i(x, y)$ and $\psi_i(\tilde{x}, \tilde{y})$ are to be estimated.

Acquiring such wide area’s micro-motion like vibration of almost rigid but deformable object surfaces requires dense observation in time and space. One promising solution is to use a camera, since it can capture wide area information at a short period of time. Optical triangulation is a common method to measure displacement from captured image, however, since the movement by vibration is much smaller than the size of the object, *i.e.*, less than one pixel, it is impossible to measure such minute motion by the method. Another approach is to use optical interferometry. Since the method uses the difference of the length of multiple light paths, the accuracy mainly depends on the wavelength of the light, which indicates that the resolution of a camera is less dependent. The disadvantage of this approach is that it requires a complicated and precise setup with many optical components to generate the high quality reference light and path.

Speckle pattern, which is a phenomenon of light interference on object surface, has also been frequently used for detecting micro-motion. Since one of important characteristics of speckle pattern is high sensitivity of its appearance, it is utilized for observing minute phenomenon, such as micro-motion of object surface. Another unique characteristic of speckle pattern is that no reference light is necessary to observe the pattern, because it is mutual interference of the lights reflected from the multiple points on object’s surface. Those characteristics enables a simple setup of devices to detect micro-motion in a wide field of view. A typical usage of speckle pattern for observing the minute movement is the frequency analysis, since the minute movement of object surface caused by vibration usually has a cyclic period, which can be effectively calculated by temporal analysis of the intensity at each pixel. One limitation of such speckle analyses is that since speckle is essentially an independent phenomenon at each pixel, it cannot extract temporal relationship, such as phase, between neighboring pixels, *i.e.*, wave propagation on object surface caused by vibration cannot

be acquired. To the best of our knowledge, such wave propagation phenomenon has not been measured yet. In this paper, we propose a method to extract such spatio-temporal information of micro-motion on the surface by analyzing speckle pattern captured by a camera. In our method, series of speckle patterns of each patch are embedded into low-dimensional space and surface parameters at each pixel are estimated by joint optimization. The contribution of the paper is summarized as follows.

- The minute movement at each point of object’s surface can be extracted as the low-dimensional embedding of laser speckle pattern.
- The spatial consistency of the embedded information is globally supported by smoothness constraint of the surface, which achieves the spatio-temporal analysis of speckle patterns.
- Various kind of wave propagation phenomena caused by vibration are first densely measured and visualized by our algorithm in real scene experiments.

2 Related work

As methods to observe minute movement of an object, four methods can be considered. First, a contact sensor such as accelerometers is typically used to measure the vibration, but this approach is not suitable for spatial analysis that needs dense observation. Non-contact methods that observe vibration by using cameras have advantage in dense observation.

Both passive and active approaches have been studied to observe minute movements of objects by using a camera. As passive approaches, the methods based on optical flows and pattern matching by correlation have been proposed to observe vibrating objects [1, 2]. Wu et al. [3] proposed a method to visualize subtle movements by magnifying the displacements based on spatio-temporal filtering. They have extended the method to recognize the sound by observing the vibration in the video [4] or the method to estimate material properties [5]. If the displacement is small, these methods need to zoom up the targets to detect the change of intensity due to their passive approach. Since passive approaches cannot be applied in the case that the vibration is smaller than the camera resolution, they have disadvantage in sensitivity.

As active approaches, laser-based methods have been proposed. When the wide field of view is illuminated by coherent laser light, Fig.1(a) is an example of speckle pattern on an object’s surface. While the power of the incident light is uniform, the dotted pattern is observed by a camera. When the surface vibrates, the pattern randomly changes as shown in the right three images, which are the zoom-up of the image patch in the red rectangle. The size of speckle depends on the aperture of the imaging system. If the aperture is large, the speckle of neighboring pixels is unrelated, and hard to distinguish from the noise of the imaging system in some cases. The irradiance of speckle pattern obeys negative exponential statistics, which indicates that some bright points exist while speckle patterns generally have many dark areas. The basic characteristics of speckle pattern have been studied in literature [6, 7].

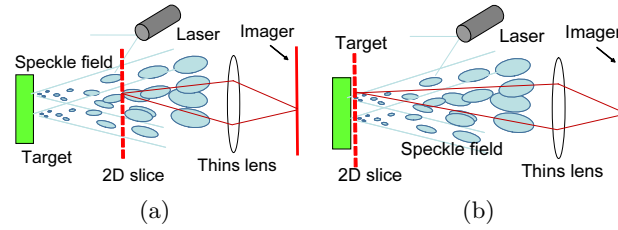


Fig. 2. The speckle field and observed 2D slices. (a) thin lens observation of fused speckle and (b) thin lens observation of independent speckle pattern.

There are two approaches to extract the information from the images of speckle. First one that calculate the phase of vibration by using speckle pattern is based on interferometry, which is called electronic speckle pattern interferometry (ESPI) [8–10]. This approach uses a reference light and compare the length of the paths between the reference light and the light from an object. If the length changes by the deformation of the object, the intensity captured by a camera changes due to the interference of two lights. In this case, the object movement is called out-of-plane motion that is along the viewing direction of the camera. The absolute displacement by the movement can be calculated by using the wavelength of the light. But since this approach requires a highly calibrated setting, it have disadvantage in simplicity of the data acquisition. García et al. [11] measured distance between object and camera by out-of-plane motions, which are not based on interferometry but needs precise calibration to obtain the speckle beforehand that corresponds to each distance.

Second approach with speckle pattern, which is called speckle photography, do not require the setup for interference. If an object slightly moves in the direction parallel to the image plane, which is called in-plane motion, the movement of speckle pattern is simple translation [12]. The motion of the object therefore can be calculated by the techniques of pattern matching. This approaches are used for estimating blood flow [13], motion sensing [14], detecting small deformation [15]. For the analysis of out-of-plane motion, Zalevsky et al. [16] proposed a method to extract the vibration caused by sound and heart beat by using speckle patterns produced by projecting a point laser. Although the periodic signal is detected by calculating the correlation of the pattern, it is single-point observation and cannot applied to spatial analysis of the vibration. Synnergren [17] proposed to combine stereo vision and speckle photography, where measuring in-plane motions using speckle photography is used for estimate disparity between stereo images. Thus, out-of-plane displacements can be estimated. The speckle motion of a front-parallel object along out-of-plane axis becomes rotationally symmetric as analyzed in [18], which can be used to estimate out-of-plane motion. The methods [19–22] to estimate combined motion including in-plane and out-of-plane motions are also proposed. Although these methods are based on tracking speckle patterns, one of the problem is that a speckle pattern drastically

change along out-of-plane motion if it is observed at the focal plane. They therefore used defocused or lens-less setups to observe moderate change of speckle. As the trade-off, the spatial resolution of the image is degraded and only a couple of motions are estimated at a time. In contrast, the method proposed in this paper observes speckles on the target surface using lens. It can obtain pixel-wise displacement information as a result, which is realized by multivariate analysis by using speckle pattern for spatial analysis of out-of-plane vibration instead of tracking pattern.

3 Overview of the method

3.1 Principle

Generally, previous speckle photography methods observe 2D slices of 3D speckle field that is far from the target surface, which is generated by interference of reflected laser, as shown in Fig.2(a). Since the speckle fields are magnified and fused, changes of the speckle pattern is analyzed as a whole. However, this makes the spatial resolution inevitably low, or large rigid motions of objects are assumed. One solution is to observe 2D slices near the object surface, where each speckle pattern is small and independent, by focusing on the target surface (Fig.2(b)).

However, there are two problems in this approach: (1) the speckle pattern near object surface drastically changes its appearance w.r.t. out-of-plane motion, and (2) if focus plane is near the target, speckle image w.r.t. out-of-plane motion becomes totally different [18], because the speckle fields from local points are not fused. Thus, analysis of this type of speckle images needs a completely different approach. To overcome the problem, the intensities in a local image patch around a pixel is considered as a feature vector of the pixel and the distance between feature vectors can be used as a metric of the similarity/difference between the slices.

3.2 System configuration and algorithm

Fig.1(b) shows a configuration of the system. A coherent laser light is reflected on multiple points on the rough surface of an object and since the reflected lights have different phases, the mutual interference occurs between them, generating speckle field. When the relative position between the surface and camera changes along the out-of-plane axis, the observed image patches change drastically according to the position of the camera relative to the object surface. Although the amplitude of speckle pattern is almost random if the number of reflected points is very large, the image patches are reproducible if the relative position is the same. The proposed method consists of the following steps.

1. Capture sequence of speckle pattern near object surface using wide aperture lens.

2. Embed the feature vector of the local patch around each pixel into nonlinear low-dimensional space.
3. Make the low-dimensional space consistent between neighboring pixels.
4. Optimize the parameters of local surface to fit the low-dimensional space.

4 Implementation

4.1 Representation of object surface

The purpose of our method is to estimate subtle motion of object surface with pixel-wise density. The surface is assumed locally planer and the proposed method estimates 3D plane parameters around each pixel (x, y) at frame i defined as follows:

$$z = [\tilde{x} - x, \tilde{y} - y, 1]\boldsymbol{\psi}_i(x, y) \quad (1)$$

where $\boldsymbol{\psi}_i(x, y) = (\psi_1, \psi_2, \psi_3)^T$ is three dimensional vector as the plane parameters, and (\tilde{x}, \tilde{y}) are neighbor pixels around (x, y) . The offset at the the origin of the local plane indicates surface displacement $d(x, y)$ as the movement at the pixel (x, y) , which is calculated by $d(x, y) = [0, 0, 1]\boldsymbol{\psi}_i(x, y) = \psi_3$. The local plane is calculated for each pixel, and Fig.1(c) shows a situation that the local patch of the plane for (x, y) and (\tilde{x}, \tilde{y}) . Since the displacement is estimated from image patches, it is determined up to scale.

4.2 Embedding speckle pattern for each pixel

To observe the movement of surface, a video is captured during the movement with projecting the coherent light generated by a laser light source. Let $I_i(x, y)$ the intensity of a pixel (x, y) at frame i of the video. The pixels (x_k, y_k) in the local image patch $P(x, y)$ forms a feature vector $\mathbf{F}_i(x, y) = (I_i(x_1, y_1), \dots, I_i(x_k, y_k))$ that describes the state of the local patch of surface. To analyze the movement between two frames i and j , the difference of two image patches is calculated by the Euclidean distance of the feature vectors.

$$D_{i,j}(x, y)^2 = \|\mathbf{F}_i(x, y) - \mathbf{F}_j(x, y)\|^2 \quad (2)$$

$$= \sum_{(x_k, y_k) \in P(x, y)} (I_i(x_k, y_k) - I_j(x_k, y_k))^2 \quad (3)$$

If the size of local patch is sufficiently large, the degree of freedom of the minute movement of the surface is much smaller than the dimension of $\mathbf{F}_i(x, y)$. It indicates that the distance is approximated by the distance of the low-dimensional vectors. Let $\boldsymbol{\Psi}_i(x, y) = (\psi_{i,1}(x, y), \dots, \psi_{i,l}(x, y))$ a low-dimensional vector of which the dimension is $l (<< k)$. Namely, the distance becomes

$$D_{i,j}(x, y)^2 = \|\boldsymbol{\Psi}_i(x, y) - \boldsymbol{\Psi}_j(x, y)\|^2 \quad (4)$$

The low-dimensional vector can be obtained by the techniques of dimensionality reduction, which embed the input vectors in the low-dimensional space so that the distance between two vectors are preserved after embedding. Since the movement is large, the speckle patterns between two frames becomes almost uncorrelated. Therefore, the relationship between the movement and the distance of speckle patterns is expected to be nonlinear. Various methods of dimensionality reduction for nonlinear distances have been proposed such as Isomap [23], locally linear embedding [24], Laplacian eigenmaps [25], diffusion maps [26] and t-SNE [27]. Diffusion maps is used in this paper.

The input for the dimensionality reduction is a set of feature vectors $\mathbf{F}_i(x, y)$ ($i = 1, \dots, N$), which are created from the local image patches around a pixel (x, y) of frames $i = 1, \dots, N$. In the experiments, the size of a patch is 11×11 pixels and the dimension of the feature vector is 11^2 . The speckle pattern of a image patch is embedded into $\Psi_i(x, y)$ by the dimensionality reduction. The embedding is applied for each pixel independently and N vectors of dimension l are obtained as the outputs. The dimension l is 5 in the experiments.

4.3 Making the embedded vectors spatially consistent

The embedded vector $\Psi_i(x, y)$ has ambiguity in its sign because the speckle has no information about the direction of the movement. Since the embedded vectors are calculated independently for each pixel by the method described in Sec.4.2, the parameters of adjacent pixels can be inconsistent each other. The second step of the proposed method is to make them spatially consistent.

A linear transformation is introduced to modify the embedded vectors as follows:

$$\psi_i(x, y) = \mathbf{M}(x, y)\Psi_i(x, y) \quad (5)$$

where $\mathbf{M}(x, y)$ is a $3 \times l$ matrix and $\Psi_i(x, y)$ is a $l \times 1$ column vector for the pixel (x, y) . Since the local plane parameters of neighbor pixels should be similar, the following constraint is satisfied to make $\psi_i(x, y)$ spatially consistent

$$\min_{\mathbf{M}} \sum_i \sum_{(x_1, y_1)} \sum_{(x_2, y_2)} E_s(i, x_1, y_1, x_2, y_2) \quad (6)$$

$$E_s(i, x_1, y_1, x_2, y_2) = \|[x_2 - x_1, y_2 - y_1, 1]\mathbf{M}(x_1, y_1)\Psi_i(x_1, y_1) - [0, 0, 1]\mathbf{M}(x_2, y_2)\Psi_i(x_2, y_2)\|^2 \quad (7)$$

where (x_1, y_1) is a point in the whole image and (x_2, y_2) is a point in the neighborhood window of (x_1, y_1) . This constraint means that the 3D local patches in Fig.1(c) have the same height at the overlapping pixels in the image. The constraint for a pair of (x_1, y_1) and (x_2, y_2) becomes

$$\begin{aligned} & (\Psi_i(x_1, y_1)[x_2 - x_1, y_2 - y_1, 1]) \circ \mathbf{M}(x_1, y_1) \\ & - (\Psi_i(x_2, y_2)[0, 0, 1]) \circ \mathbf{M}(x_2, y_2) = \mathbf{0} \end{aligned} \quad (8)$$

where \circ is element-wise product. Let \mathbf{m} the column vector by stacking $\mathbf{M}(x, y)$ for all pixels after vectorization. Since the constraints are expressed by $\mathbf{A}\mathbf{m} = \mathbf{0}$, where \mathbf{A} is the coefficient matrix calculated from Eq.(8), \mathbf{m} is given as the eigenvector associated with the smallest eigenvalue of $\mathbf{A}^T\mathbf{A}$. Once $\mathbf{M}(x, y)$ is calculated, the modified embedded vectors $\boldsymbol{\psi}_i(x, y)$ calculated by Eq.(5) become spatially consistent. Note that the ambiguity of the movement direction in total remains due to the ambiguity of the eigenvector even after making it spatially consistent.

One of the problem in calculating the eigenvector is that the temporal distribution of $\boldsymbol{\Psi}_i(x, y)$ between pixels is different. If $\boldsymbol{\Psi}_i(x, y)$ of a pixel (x, y) is almost zero, the magnitude of $\mathbf{M}(x, y)$ is nearly equal to one and the parameters for other pixels become almost zero, because $\boldsymbol{\psi}_i(x, y)$ does not affect the error even if the magnitude of $\mathbf{M}(x, y)$ is dominant in the eigenvector. Therefore, the standard deviation of $\boldsymbol{\Psi}_i(x, y)$ is normalized before calculating the coefficient matrix \mathbf{A} along the time axis as follows:

$$\Psi'_{ik} = \Psi_{ik}/(\sigma_k + \epsilon), \quad \sigma_k^2 = \frac{1}{N} \sum_i (\Psi_{ik} - \bar{\Psi}_k)^2 \quad (9)$$

where Ψ_{ik} is the k -th component of $\boldsymbol{\Psi}_i$, $\bar{\Psi}_k$ is the mean value of Ψ_{ik} and ϵ is a small number to avoid division by zero.

Since the cost of calculating the eigenvector in high resolution is large, $\mathbf{M}(x, y)$ is calculated after subsampling pixels. In the experiments, the original image is 512×512 pixels and subsampled to 64×64 pixels.

4.4 Optimizing surface parameters

The calculation of $\mathbf{M}(x, y)$ in Sec.4.3 does not consider the distance between the features calculated by Eq.(2). In the third step, $\mathbf{M}(x, y)$ is optimized so that the embedded vector preserves the distance of the features.

By assuming the movement between adjacent two frames is sufficiently small, the constraint so that the distance of the embedded vectors preserves the distance of the features is added to the error function to be minimized as follows:

$$\min_{\mathbf{M}} \sum_i \left[\sum_{(x,y)} E_t(i, x, y) + \lambda \sum_{(x_1, y_1)} \sum_{(x_2, y_2)} E_s(i, x_1, y_1, x_2, y_2) \right] \quad (10)$$

$$E_t(i, x, y) = (\| \boldsymbol{\psi}_i(x, y) - \boldsymbol{\psi}_{i+1}(x, y) \| - \| \mathbf{F}_i(x, y) - \mathbf{F}_{i+1}(x, y) \|)^2 \quad (11)$$

where E_s is the spatial constraint defined by Eq.(7) and λ is its weight. Once the transformation matrix $\mathbf{M}(x, y)$ is optimized, the plane parameter $\boldsymbol{\psi}_i(x, y)$ is obtained, and The displacement for each pixel is given as the third component of $\boldsymbol{\psi}_i(x, y)$.

The initial guess $\boldsymbol{\psi}'_i(x, y)$ for nonlinear minimization of Eq.(10) is given by $\boldsymbol{\psi}_i(x, y)$ calculated in Sec.4.3 after normalizing the magnitude for each pixel as

follows:

$$\boldsymbol{\psi}'_i(x, y) = \frac{m_F}{m_\psi + \epsilon} \boldsymbol{\psi}_i(x, y) \quad (12)$$

$$m_\psi = \frac{1}{N} \sum_i \|\boldsymbol{\psi}_i(x, y) - \boldsymbol{\psi}_{i+1}(x, y)\|^2 \quad (13)$$

$$m_F = \frac{1}{N} \sum_i \|\mathbf{F}_i(x, y) - \mathbf{F}_{i+1}(x, y)\|^2 \quad (14)$$

Since $\mathbf{M}(x, y)$ calculated in Sec.4.3 is subsampled, $\mathbf{M}(x, y)$ is interpolated before optimizing parameters to obtain the displacement for the image of the original resolution. It is done by interpolating the displacement of the subsampled images calculated by using the initial guess $\boldsymbol{\psi}'_i(x, y)$. Let $d(x, y)$ the linearly interpolated displacement at the pixel (x, y) of the original resolution. $\mathbf{M}(x, y)$ at the interpolated pixels should satisfy the following equation for the neighboring pixels (\tilde{x}, \tilde{y}) :

$$[\tilde{x} - x, \tilde{y} - y, 1] \mathbf{M}(x, y) \boldsymbol{\Psi}_i(x, y) = d(\tilde{x}, \tilde{y}) \quad (15)$$

Since this linear equation of $\mathbf{M}(x, y)$ is obtained for all pixels in the local patch, $\mathbf{M}(x, y)$ is calculated as the least-square solution. Once $\mathbf{M}(x, y)$ is obtained for all pixels, the optimization is applied with the images of the original resolution.

5 Experiments

In the experiments, we used a high-speed monochrome camera that captures images at more than 1000 frames/second and a laser light source as the incident light to produce the speckle pattern. The resolution of the camera is 512×512 pixels. The light source and camera have about 40 degrees field of view.

5.1 Evaluating the calculated displacement with respect to the real offset

The first experiment is to evaluate the displacement calculated by the proposed method with the images by changing the position with known offsets. Fig.3(a) shows the experimental setup. A planar object is illuminated by a laser projector and is observed by a camera. The camera is mounted on a microstage and the position is moved along the camera axis. A set of 100 images are obtained in total by capturing five images at each offset during changing the offset from 0 to $18 \mu\text{m}$ every $1 \mu\text{m}$. The proposed method described in Sections 4.2 and 4.3 is applied to the set of 100 images since the order of images cannot be used for the optimization for this dataset. In this experiment, we evaluate if the displacement calculated by the proposed method has linear relationship compared to the offset given by the microstage. Since speckle can be observed if an object has rough surface, three types of materials (wood, cardboard and sponge) are tested in this

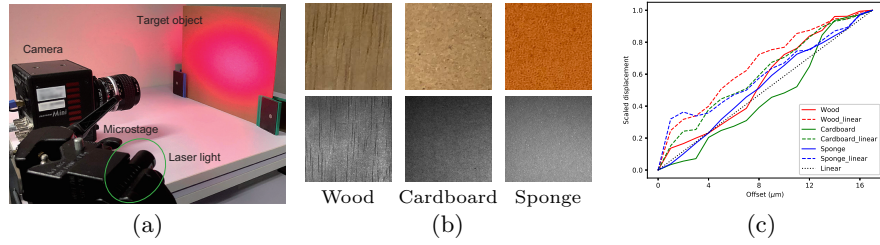


Fig. 3. (a) A planar object is illuminated by a laser light source and observed by a camera mounted on a microstage, which moves the camera along the axis. (b) Three materials (wood, cardboard, sponge) are tested. The images in the upper row are illuminated by room light, and the ones in the lower row are illuminated by laser light. (c) The relationship between the calculated displacements and the real offsets are shown. The displacements are scaled from 0.0 to 1.0.

experiment to evaluate the relationship between the calculated displacement and the real offset.

Fig.3(c) shows the results of the calculated displacements. Since the absolute values of displacements can not be obtained by the proposed method, the values are scaled from 0.0 to 1.0, which correspond from 0 to 18 μm of the real offset. The displacements are averaged at each offset. The results are compared with the linear approach calculating Euclidean distance between the patches of zero offset and the others. The root-mean-square errors of the displacements from the linear relationship are 0.080, 0.076 and 0.038 for the three materials, wood, cardboard and sponge, in the scaled displacement. The values correspond to 1.36 μm , 1.28 μm and 0.64 μm in the real scale. The root-mean-square errors of the linear approach are 0.171, 0.108 and 0.118 in the scaled displacement, and 2.91 μm , 1.83 μm and 2.01 μm in the real scale, respectively. These results show the proposed method is applicable for various materials to discriminate the minute displacements and the relationship with respect to the real movement is close to linear than by using linear distance.

5.2 Comparison with accelerometers

Second, the proposed method is tested for a case of dynamic movement. The result is compared to the measurements by the accelerometers. Fig.4 shows the setup in the experiments. The distance from the camera to the target object (wood panel) is about 1m, and the field of view is about 0.6m square at the target's position. The object is in contact with a speaker as the vibration source, which generates a 60Hz sine wave. The direction of the vibration is nearly parallel to the viewing direction and the movement is out-of-plane. The image sequence of 256 frames is captured by a high speed camera at 1000 frames/second. Two accelerometers are placed on the object to measure the vibration and compare with the results by the proposed method.

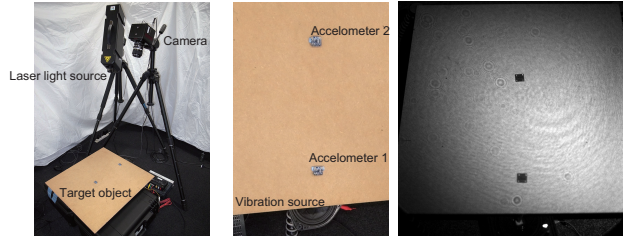


Fig. 4. The experimental setup consists of a camera and laser light source. A speaker is used as a source to vibrate the target object. Two accelerometers are placed on the object to measure the vibration. The right image is one of input images illuminated by the laser light.

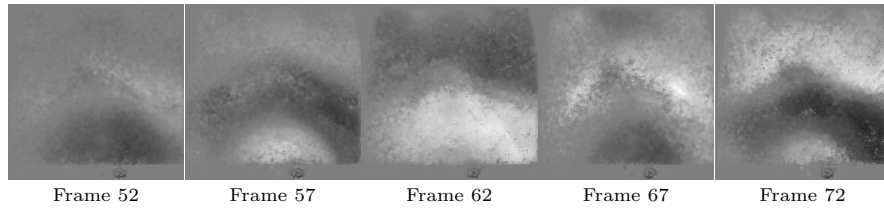


Fig. 5. The calculated displacements are shown for five frames in the sequence. The displacements are indicated by the brightness in these images.

Fig.5 shows the results of calculated displacement of five frames in the image sequence. The area of the same brightness indicates the same displacement. The vibration propagated from the bottom of the image at the beginning, and became a standing wave in the latter part. The measurements by the proposed method is compared to the values calculated by integrating the acceleration twice. Fig.6 shows the comparison with two measurements. Since the proposed method cannot calculate the absolute values of displacement, it is scaled to fit the mean magnitude of the measurements by the accelerometers. The two accelerometers are placed at the different distance from the vibration source. The accelerometer 2 is delayed about the half of the cycle from the accelerometer 1. The results by the proposed method is synchronized with the measurements by the both accelerometers. The normalized cross correlation of the signals between the proposed method and the accelerometers are 0.768 and 0.863. The high correlation indicates the proposed method can extract the phase of the minute vibration from the speckle pattern. Fig.7 shows the power spectrum of the vibration measured by the accelerometers and the proposed method. A strong peak at the same frequency is observed in all the results. Fig.8 shows the vertical slices of the displacements along the center line of the images of the two frames in Fig.5. Since the spatial consistency of the displacements calculated for each pixel in-

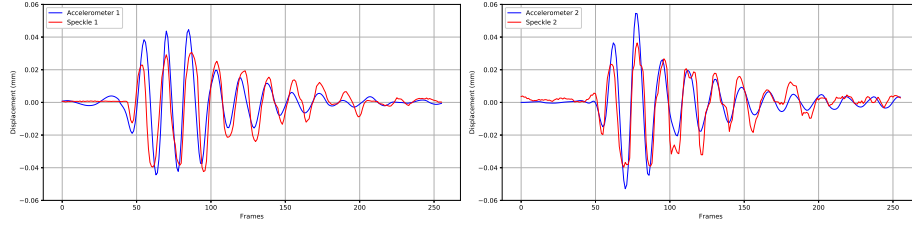


Fig. 6. The measurements by two accelerometers are compared to the results by the proposed method.

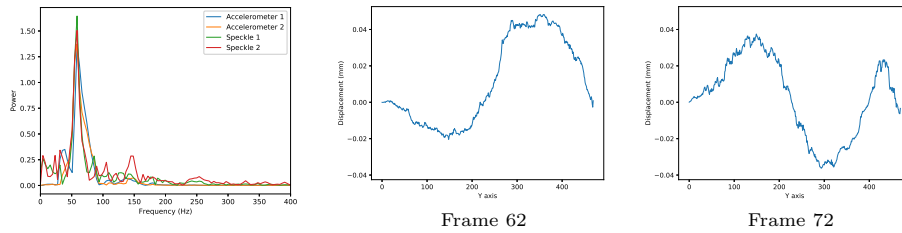


Fig. 7. The power spectrum

Fig. 8. The vertical slices of the displacements

independently in Sec.4.2 is obtained by the method described in Sec.4.3, the wave propagated in the image can be observed by the displacements.

5.3 Visualizing various movements

Third, the proposed method is applied to various movements of different materials. In Fig.9, a finger touches the canvas cloth and the movement occurs from the touching points. The movement propagates as a circular wave, which is reflected at the edge of the canvas. The left image in Fig.9 shows one of the image sequences of the input images and the rest is the resulting displacement images. The images are captured at 1000 frames / second in this experiment. The canvas is pushed down by the finger at first and the position returns back after releasing the touch. The canvas cloth vibrates repeatedly during the touch.

Next, a hammering experiment of a wall made of metal panel is observed by the proposed method. The wall is painted and the speckle can be observed on the surface. Fig.10(a) shows the situation and one of the input images. In this experiment, the camera equips the band-pass filter to capture the infrared laser light and discard the illumination by room light. The image sequence is captured at 6400 frames/second in this experiment. Fig.11 shows the displacements for four frames in the sequence. The wave started from the hitting point and propagated the metal wall. Since the size of wall is known and the speed of the wave

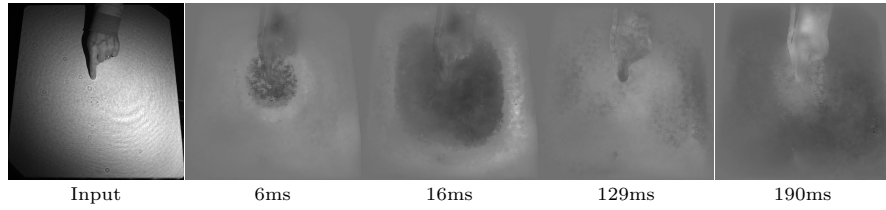


Fig. 9. The movement is produced by touching the canvas by a finger in this sequence. The movement starts from the touching point, and propagates as a circular wave.

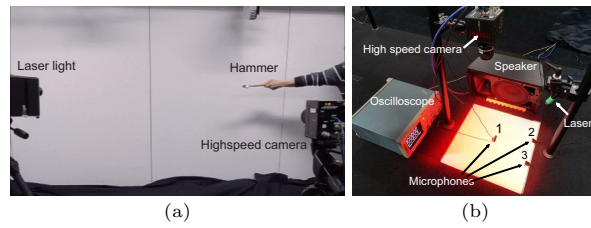


Fig. 10. Experimental setups: (a) The experiment of hitting a painted metal wall by a hammer. (b) The experiment of visualizing sound wave.

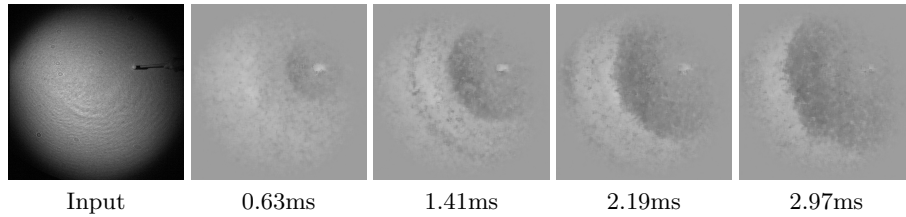


Fig. 11. The displacements generated by hammering are calculated.

is about 17.5 pixel/frame, the speed of wave that propagates in the metal wall is about 250 m/s.

Finally, to visualize a sound wave, we set up a speaker and placed tissue papers that vibrates with the sound which propagates through the air. The tissue papers are fixed to the floor with tapes as shown in the setup image in Fig.10(b) and captured by the high-speed camera with 10,000fps. We also put three microphones to obtain ground truth data. The distances from the speaker to the microphones are 34cm, 32cm and 46cm, respectively. Since the floor is hard enough, the tissue papers' motion is considered to be caused only by the air. The observed displacements are shown in Fig.12. The wave-front propagates from the right to the left in wide images.

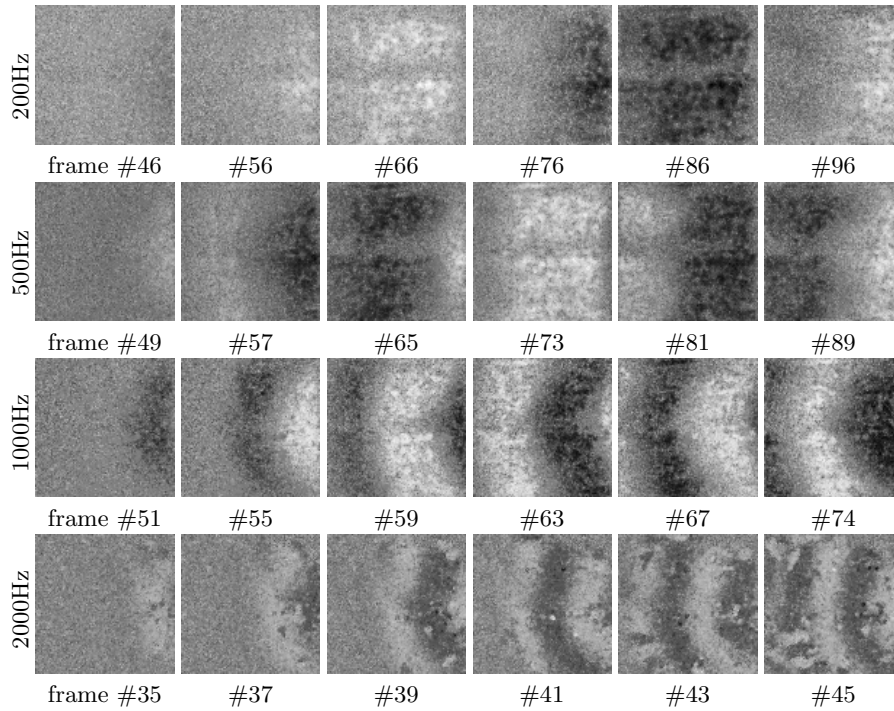


Fig. 12. Visualization of sound wave. Tissue papers are fixed to the floor with tapes, and a sound speaker is placed on the right of the images. The sound wave that propagates through the air moves the papers from the right to the left.

6 Conclusion

This paper proposed a method to observe the minute movement of objects by using the speckle that is generated by the illumination of laser light. Since the speckle varies sensitively to the out-of-plane movement, it enables to detect the minute movement of objects. Calculating the displacement without complex optical setup and calibration is realized based on the approach of embedding speckle pattern to low-dimensional space. The embedded vectors, which is calculated for each pixel independently, are made spatially consistent by estimating transformation matrices. The displacement is calculated by the consistent embedded vectors. In the experiments, the calculated displacement is compared to the movement measured by a micro-stage and accelerometers. Although the propose method cannot determine the scale of the movement, it can discriminate the displacement in micrometer accuracy. The proposed method is applied to various movement and materials, and succeeded to observe the minute movement of the objects. In future work, we plan to extend the proposed method to measure the real scale of the movement with simple and easy calibration.

References

1. D’Emilia, G., Razzè, L., Zappa, E.: Uncertainty analysis of high frequency image-based vibration measurements. *Measurement* **46** (2013) 2630–2637
2. Caetano, E., Silva, S., Bateira, J.: A vision system for vibration monitoring of civil engineering structures. *Experimental Techniques* (2011) 74–82
3. Wu, H.Y., Rubinstein, M., Shih, E., Guttag, J., Durand, F., Freeman, W.: Eulerian video magnification for revealing subtle changes in the world. *ACM Trans. Graph.* (Proceedings SIGGRAPH 2012) **31** (2012)
4. Davis, A., Rubinstein, M., Wadhwa, N., Mysore, G., Durand, F., Freeman, W.: The visual microphone: Passive recovery of sound from video. *ACM Transactions on Graphics (Proc. SIGGRAPH)* **33** (2014) 79:1–79:10
5. Davis, A., Bouman, K., Chen, J., Rubinstein, M., Durand, F., Freeman, W.: Visual vibrometry: Estimating material properties from small motions in video. *IEEE TPAMI* **39** (2017) 732–745
6. Goodman, J.: Some fundamental properties of speckle. *JOSA* **66** (1976) 1145–1150
7. Dainty, C., ed.: *Laser Speckle and Related Phenomena*. 2 edn. Springer-Verlag (1984)
8. Løkberg, O., Høgmoen, K.: Vibration phase mapping using electronic speckle pattern interferometry. *Applied Optics* **15** (1976) 2701–2704
9. Creath, K.: Phase-shifting speckle interferometry. *Applied Optics* **24** (1985) 3053–3058
10. Bavigadda, V., Mihaylova, E., Jallapuram, R., Toal, V.: Vibration phase mapping using holographic optical element-based electronic speckle pattern interferometry. *Optics and Lasers in Engineering* **50** (2012) 1161–1167
11. García, J., Zalevsky, Z., García-Martínez, P., Ferreira, C., Teicher, M., Beiderman, Y.: Three-dimensional mapping and range measurement by means of projected speckle patterns. *applied Optics* **47** (2008) 3032–3040
12. Yamaguchi, I.: Real-time measurement of in-plane translation and tilt by electronic speckle correlation. *Jpn. J. Appl. Phys.* **19** (1980) L133
13. Fujii, H., Nohira, K., Yamamoto, Y., Ikawa, H., Ohura, T.: Evaluation of blood flow by laser speckle image sensing, part 1. *Appl. Opt.* **26** (1987) 5321–5325
14. Zizka, J., Olwal, A., Raskar, R.: Specklesense: fast, precise, low-cost and compact motion sensing using laser speckle. In: *Proc. the 24th annual ACM symposium on User interface software and technology*. (2011) 489–498
15. Chang Shih, Y., Davis, A., W. Hasinoff, S., Durand, F., Freeman, W.: Laser speckle photography for surface tampering detection. In: *Proceedings / CVPR, IEEE Computer Society Conference on Computer Vision and Pattern Recognition*. (2012) 33–40
16. Zalevsky, Z., Beiderman, Y., Margalit, I., Gingold, S., Teicher, M., Mico, V., Garcia, J.: Simultaneous remote extraction of multiple speech sources and heart beats from secondary speckles pattern. *Opt Express* **17** (2009) 21566–21580
17. Synnnergren, P.: Measurement of three-dimensional displacement fields and shape using electronic speckle photography. *OptEn* **36** (1997) 2302–2310
18. Jakobsen, M.L., Yura, H., Hanson, S.G.: Spatial filtering velocimetry of objective speckles for measuring out-of-plane motion. *Applied optics* **51** (2012) 1396–1406
19. Jacquot, P., Rastogi, P.K.: Speckle motions induced by rigid-body movements in free-space geometry: an explicit investigation and extension to new cases. *Applied Optics* **18** (1979) 2022–2032

20. Jo, K., Gupta, M., Nayar, S.K.: Spedo: 6 dof ego-motion sensor using speckle defocus imaging. In: Proceedings of the IEEE International Conference on Computer Vision. (2015) 4319–4327
21. Smith, B.M., Desai, P., Agarwal, V., Gupta, M.: Colux: Multi-object 3d micro-motion analysis using speckle imaging. *ACM Transactions on Graphics (TOG)* **36** (2017) 1–12
22. Smith, B.M., O’Toole, M., Gupta, M.: Tracking multiple objects outside the line of sight using speckle imaging. In: Proceedings of the IEEE Conference on Computer Vision and Pattern Recognition. (2018) 6258–6266
23. Tenenbaum, J.B., De Silva, V., Langford, J.C.: A global geometric framework for nonlinear dimensionality reduction. *science* **290** (2000) 2319–2323
24. Roweis, S.T., Saul, L.K.: Nonlinear dimensionality reduction by locally linear embedding. *science* **290** (2000) 2323–2326
25. Belkin, M., Niyogi, P.: Laplacian eigenmaps for dimensionality reduction and data representation. *Neural computation* **15** (2003) 1373–1396
26. Coifman, R.R., Lafon, S.: Diffusion maps. *Applied and computational harmonic analysis* **21** (2006) 5–30
27. Maaten, L.v.d., Hinton, G.: Visualizing data using t-sne. *Journal of machine learning research* **9** (2008) 2579–2605